

# A theoretical investigation of the specific heat of superlattices in a magnetic field

R. Mélin<sup>(1)\*</sup> and F. Fominaya<sup>(2)†</sup>

<sup>(1)</sup> International School for Advanced Studies (SISSA), Via Beirut 2–4, 34014 Trieste, Italy

<sup>(2)</sup> CRTBT–CNRS, 25 Avenue des Martyrs, BP 166X, 38042 Grenoble CEDEX, France

February 4, 2017

## Abstract

We analyze the specific heat variations as a function of an external magnetic field of a simple model of superlattice that includes (i) in-plane ferromagnetic exchange, (ii) interplane ferromagnetic exchange, (iii) dipolar interactions, (iv) magnetocrystalline anisotropy. The calculations are carried out at the spin wave level. The interplay between the existence of a canting transition and the anisotropy of the structure generate non trivial behavior for the spin wave contribution to the low temperature specific heat as a function of an external magnetic field when dipolar interactions and magnetocrystalline anisotropy are taken into account.

---

\*e-mail: melin@crtbt.polycnrs-gre.fr

†e-mail: fominaya@labs.polycnrs-gre.fr

## 1 Introduction

Magnetic multilayers made of alternating ferromagnetic films and non magnetic films (being the typical thickness of these films several atomic monolayers) present interesting properties in the presence of an external magnetic field, as for instance the giant magnetoresistance effect found in [1] and also in other multilayers [2]. Up to now, many different measurements have been performed [3][4], but to our knowledge, the specific heat of magnetic multilayers has never been studied due to the experimental difficulty of measuring a mass as little as a  $\mu\text{g}$ . Recent developments in nanocalorimetry allow now to achieve the necessary resolution for such a measurement [5], [6]. The aim of this article is to present a theoretical investigation of the low temperature specific heat of bulk multilayers. Two contributions to the specific heat are present: first, the contribution of paramagnetic layers and second, a small contribution of spin waves. We analyze here the variations of the low temperature spin wave contribution as a function of the strength of magnetic field applied perpendicular to the planes or parallel to the planes. This contribution could possibly be measured via a high accuracy specific heat measurement. Our goal is not to obtain quantitative accurate results, but rather to give a scenario for the behavior of the spin wave excitations and the consequences for the spin wave contribution to the specific heat.

We thus work with a simple model including (i) in-plane ferromagnetic exchange of the order of  $J_{\parallel} \simeq 100$  K. (ii) interplane antiferromagnetic exchange of the order of  $J_{\perp} \simeq 1$  K. (iii) in-plane dipolar interactions with a strength  $J_d$  of the order  $J_d \simeq 1$  K. (iv) magnetocrystalline anisotropy of the order  $K \simeq 0.5$  K. The magnetic moments are taken to be localized. This is only an approximation, but widely used in the literature (see for instance [8]). For simplicity, we study the magnetic multilayers as a bulk system, and we use periodic boundary conditions in each direction. In particular, we do not take into account the surface spin wave modes (see reference [8] and references therein). Even at this level of approximation, we find a non trivial behavior for the spin wave part of the specific heat, associated to the transition from a canted spin configuration to an aligned spin configuration as the strength of the magnetic field increases. This transition was already noticed (see [8] and references therein). We also find that, when dipolar interactions and anisotropy are taken into account, the anisotropy of the structure implies an anisotropy of the specific heat with respect to the magnetic field direction. Namely, the specific heat with a perpendicular magnetic field is larger than the specific heat with an in-plane magnetic field.

## 2 Description of the model

Let us now describe the model and fix the notations. The  $x$  and  $y$  axis are chosen parallel to the layers and the  $z$  axis is perpendicular to the layers. Since we are interested in bulk properties, we use periodic boundary conditions in each direction. Moreover, the spins lie on a cubic lattice. The

Hamiltonian reads

$$H = -\frac{1}{2} \sum_{\mathbf{x}, \mathbf{x}'} \mathbf{S}_{\mathbf{x}} \cdot \Lambda(\mathbf{x}, \mathbf{x}') \cdot \mathbf{S}_{\mathbf{x}'} - \mathbf{h} \cdot \sum_{\mathbf{x}} \mathbf{S}_{\mathbf{x}}, \quad (1)$$

where the exchange tensor  $\Lambda$  is

$$\Lambda_{\alpha, \beta}(\mathbf{x}, \mathbf{x}') = J_{\parallel} \delta_{\alpha, \beta} \left( \delta_{\mathbf{x}, \mathbf{x}' + \mathbf{e}_x} + \delta_{\mathbf{x}, \mathbf{x}' - \mathbf{e}_x} + \delta_{\mathbf{x}, \mathbf{x}' + \mathbf{e}_y} + \delta_{\mathbf{x}, \mathbf{x}' - \mathbf{e}_y} \right) \quad (2)$$

$$- J_{\perp} \delta_{\alpha, \beta} \left( \delta_{\mathbf{x}, \mathbf{x}' + \mathbf{e}_z} + \delta_{\mathbf{x}, \mathbf{x}' - \mathbf{e}_z} \right) - J_d d_{\alpha, \beta}(\mathbf{x}, \mathbf{x}') \delta_{z, z'} \quad (3)$$

$$+ K d_{\alpha, \beta}(\mathbf{x}, \mathbf{x}') \left( \delta_{\mathbf{x}, \mathbf{x}' + \mathbf{e}_x} + \delta_{\mathbf{x}, \mathbf{x}' - \mathbf{e}_x} + \delta_{\mathbf{x}, \mathbf{x}' + \mathbf{e}_y} + \delta_{\mathbf{x}, \mathbf{x}' - \mathbf{e}_y} \right) \delta_{z, z'}, \quad (4)$$

the dipolar tensor being

$$d_{\alpha, \beta}(\mathbf{x}, \mathbf{x}') = \frac{1}{|\mathbf{x}' - \mathbf{x}|^3} \left( \delta_{\alpha, \beta} - 3 \hat{\mathbf{u}}_{\alpha}(\mathbf{x}, \mathbf{x}') \cdot \hat{\mathbf{u}}_{\beta}(\mathbf{x}, \mathbf{x}') \right). \quad (5)$$

$\mathbf{e}_x, \mathbf{e}_y, \mathbf{e}_z$  are the unit vectors in the  $x, y$  and  $z$  directions, and  $\hat{\mathbf{u}}(\mathbf{x}, \mathbf{x}')$  is the unit vector in the direction  $\mathbf{x}' - \mathbf{x}$ . In equation (1),  $\mathbf{h}$  is an external magnetic field. In order to make contact with the literature, one should remember that  $h$  is related to the "true" magnetic field  $H$  by  $h = MH$ , with  $M$  the net magnetic moment. As far as dipolar interactions are concerned, we take into account only in-plane dipolar interactions. This is justified by the structure of magnetic multilayers: the ferromagnetic layers are separated by paramagnetic layers, so that it is reasonable, in a first approximation, to assume that dipolar interactions are long ranged inside a layer and that two spins in a different layer do not experience dipolar interactions.

The term (4) is a magnetocrystalline anisotropy term, modeled via a short range pseudo dipolar interaction, as proposed in [9]. We choose the anisotropy to be small enough so that in a zero magnetic field the magnetization is in the planes. This amounts to consider only the case of magnetic multilayers for which the thickness of the ferromagnetic layers is large enough [10], typically larger than 20 Å.

### 3 Spin wave spectrum in a zero magnetic field without dipolar interactions and anisotropy

This section is devoted to the zero magnetic field case. We determine the spin wave spectrum in a zero magnetic field and show that, due to the three dimensionality of the system, no divergences appear at the spin wave level (unlike the one dimensional Heisenberg chain case).

#### 3.1 Spin wave spectrum

We first analyze the zero magnetic field spin wave spectrum and the specific heat of the "minimal" model including only the ferromagnetic  $J_{\parallel}$  and antiferromagnetic  $J_{\perp}$  exchange constants. This model in a zero magnetic field can be solved at the spin wave level using the Holstein–Primakov bosons

method [11]. Introducing two types of bosons  $a$  and  $b$  for each type of layer, keeping as usually only the  $1/s$  leading quantum corrections in the semi classical (large  $s$ ) approach and Fourier transforming the Hamiltonian leads to

$$H = \sum_{\mathbf{q}} A_{\mathbf{q}} (a_{\mathbf{q}}^+ a_{\mathbf{q}} + b_{\mathbf{q}}^+ b_{\mathbf{q}}) + B_{\mathbf{q}} (a_{\mathbf{q}} b_{-\mathbf{q}} + a_{\mathbf{q}}^+ b_{-\mathbf{q}}^+), \quad (6)$$

with

$$A_{\mathbf{q}} = J_{\parallel} (2 - \cos q_x - \cos q_y) + J_{\perp} \quad (7)$$

$$B_{\mathbf{q}} = J_{\perp} \cos q_z. \quad (8)$$

The Hamiltonian is readily diagonalized via the following Bogoliubov transformation

$$c_{\mathbf{q}} = \cosh \varphi_{\mathbf{q}} a_{\mathbf{q}} - \sinh \varphi_{\mathbf{q}} b_{-\mathbf{q}}^+ \quad (9)$$

$$d_{\mathbf{q}} = \cosh \varphi_{\mathbf{q}} b_{\mathbf{q}} - \sinh \varphi_{\mathbf{q}} a_{\mathbf{q}}^+, \quad (10)$$

with  $\tanh(2\varphi_{\mathbf{q}}) = -B_{\mathbf{q}}/A_{\mathbf{q}}$ , leading to the following spin-wave spectrum  $\omega_{\mathbf{q}}^2 = A_{\mathbf{q}}^2 - B_{\mathbf{q}}^2$ :

$$\omega_{\mathbf{q}}^2 = (J_{\parallel}(2 - \cos q_x - \cos q_y) + J_{\perp})^2 - J_{\perp}^2 \cos^2 q_z. \quad (11)$$

If  $J_{\parallel} = 0$ , we recover the spin-wave spectrum  $\omega_{\mathbf{q}} = J_{\perp} |\sin q_z|$  of the Heisenberg chain [12] [13] and if  $J_{\perp} = 0$ , we recover the  $\omega_{\mathbf{q}} = J_{\parallel}(2 - \cos q_x - \cos q_y)$  spectrum of the two-dimensional ferromagnet [13].

### 3.2 Stability of the classical alternate ground state

Before going further, we would like to show that the antiferromagnetic perpendicular exchange  $J_{\perp}$  does not destabilize the alternate ground state, unlike the one-dimensional case where the Néel state is destabilized by the first quantum corrections. The stability in the multilayer case is due to the three dimensionality of the structure. We calculate the first quantum corrections to the magnetization. To do so, we notice that

$$\langle a_{\mathbf{q}}^+ a_{\mathbf{q}} \rangle = \frac{1}{2} \left( \frac{1}{\sqrt{1 - \tanh^2(2\varphi_{\mathbf{q}})}} - 1 \right), \quad (12)$$

leading to the average quantum correction  $\Delta M$  to the magnetization per spin in a layer:

$$\Delta M = -\frac{1}{(2\pi)^3} \int_{BZ} d\mathbf{q} \left( \frac{1}{\sqrt{1 - \tanh^2(2\varphi_{\mathbf{q}})}} - 1 \right), \quad (13)$$

where BZ denotes an integral over the first Brillouin zone. This integral is infrared convergent:

$$\Delta M \sim -\frac{1}{(2\pi)^3} \int_{BZ} d\mathbf{q} \frac{1}{\sqrt{q_z^2 + \frac{J_{\parallel}}{J_{\perp}}(q_x^2 + q_y^2)}}, \quad (14)$$

where we have expanded the  $A_{\mathbf{q}}$  and  $B_{\mathbf{q}}$  in the small  $\mathbf{q}$  limit. A dimensional analysis shows that  $\Delta M \sim J_{\perp}/J_{\parallel}$ . In the limit  $J_{\parallel} \rightarrow 0$ , we recover the spin-wave divergence of the Heisenberg chain [12]. In the multilayers,  $J_{\parallel}$  is two orders of magnitude larger than  $J_{\perp}$ : our spin wave approach is thus consistent from the point of view of the absence of divergences of the spin wave theory. On the other hand, the three-dimensionality of the structure also avoids problems related to the Mermin–Wagner theorem in two dimensions at a finite temperature (absence of spontaneous order in two dimension for continuous spins). We have shown the consistency of our spin wave approach only in the case of a zero magnetic field and without dipolar interactions. However, the spin wave approach is still consistent in the presence of a magnetic field and with dipolar interactions.

## 4 Spin wave theory in a perpendicular magnetic field

### 4.1 Classical ground state without dipolar interactions and anisotropy

We are first going to examine the spin wave theory when an external magnetic field is switched on, but in the absence of dipolar interaction and anisotropy. The effect of dipolar and anisotropy interactions will be discussed later on. At the classical level, the zero temperature ground state corresponds to the condition that each spin is exactly aligned in its local field. Because of the translational invariance, each spin in a given layer points in the same direction (at the classical level and at zero temperature). We denote by  $\mathbf{n}^{(a)}$  the spin vector in layers of type (a), and  $\mathbf{n}^{(b)}$  the spin vector in (b) type layers: the spins can be canted in a layer by layer fashion. Layers (a) and (b) are alternating along the  $z$  direction. The local field  $\mathbf{h}^{(a),(b)}$  in layers (a) and (b) respectively is given by

$$\mathbf{h}^{(a)} = \mathbf{h} + 2J_{\parallel}\mathbf{n}^{(a)} - J_{\perp}\mathbf{n}^{(b)} \quad (15)$$

$$\mathbf{h}^{(b)} = \mathbf{h} + 2J_{\parallel}\mathbf{n}^{(b)} - J_{\perp}\mathbf{n}^{(a)}, \quad (16)$$

where  $\mathbf{h}$  is the external magnetic field. We denote by  $\mathbf{u}$  the unit vector in the direction of the external magnetic field:  $\mathbf{h} = |h|\mathbf{u}$ . We are looking for a classical ground state such as  $\mathbf{n}^{(a)}$ ,  $\mathbf{n}^{(b)}$  and  $\mathbf{u}$  are coplanar. As we will see below, such a classical spin configuration exists. We denote by  $\alpha$  the angle between the vectors  $\mathbf{u}$  and  $\mathbf{n}^{(a)}$ :  $\mathbf{n}^{(a)} = \mathbf{u}\cos\alpha + \mathbf{v}\sin\alpha$ , where  $\mathbf{v}$  is a vector orthogonal to  $\mathbf{u}$ . The angle  $\alpha$  between the magnetic field and the spin direction is called the canting angle in what follows. The local field  $\mathbf{h}^{(a)}$  experienced by a spin in a type (a) layer is easily expressed as

$$\mathbf{h}^{(a)} = \mathbf{u} \left( h + (2J_{\parallel} - J_{\perp}) \cos\alpha \right) + \mathbf{v} \left( 2J_{\parallel} + J_{\perp} \right) \sin\alpha = |\mathbf{h}^{(a)}| (\mathbf{u}\cos\alpha + \mathbf{v}\sin\alpha). \quad (17)$$

The last equality simply means that, at the classical level, the spins are aligned with their local field. We can thus determine the direction of the  $\mathbf{n}^{(a)}$  vector:

$$\begin{aligned} \cos\alpha &= h/2J_{\perp} & \text{if } h \leq 2J_{\perp} \\ \alpha &= 0 & \text{if } h \geq 2J_{\perp}. \end{aligned} \quad (18)$$

At the classical level, the spins are thus exactly aligned with the magnetic field provided the intensity of the magnetic field is larger than  $2J_{\perp}$  and in the absence of dipolar interactions and anisotropy.

## 4.2 Spin waves spectrum without dipolar interactions and anisotropy

In the absence of dipolar interactions and anisotropy, the classical canted configuration of spins is given by (18). The in-plane spin wave degrees of freedom decouple from the perpendicular degrees of freedom. The contribution of the in-plane spin wave degrees of freedom is a trivial ferromagnetic term, which will be added at the end of the calculation. For the moment we consider only spin wave excitations along the  $z$  direction, that is, we are going to solve the Heisenberg chain with an antiferromagnetic exchange  $J_\perp$  in a magnetic field at the spin wave level. In order to obtain the appropriate excitations, we first need to express the spin operators  $\hat{\sigma}^{\pm,z}$  in terms of the rotated spin operators  $\hat{\sigma}_R^{\pm,z}$  corresponding to a spin quantization along the direction of the classical ground state. The rotated spin states are

$$|+\rangle_R = \cos\left(\frac{\alpha}{2}\right)|+\rangle - i \sin\left(\frac{\alpha}{2}\right)|-\rangle \quad (19)$$

$$|-\rangle_R = \cos\left(\frac{\alpha}{2}\right)|-\rangle - i \sin\left(\frac{\alpha}{2}\right)|+\rangle, \quad (20)$$

where the rotated spin states  $|\pm\rangle_R$  are deduced from the  $|\pm\rangle$  states by a rotation of angle  $\alpha$  around the  $x$  axis. This allows us to express the spin operators in the laboratory framework in terms of the spin operators in the local framework:

$$\hat{\sigma}^+ = -\frac{i}{2} \sin \alpha \hat{\sigma}_R^z + \cos^2(\alpha/2) \hat{\sigma}_R^+ + \sin^2(\alpha/2) \hat{\sigma}_R^- \quad (21)$$

$$\hat{\sigma}^- = \frac{i}{2} \sin \alpha \hat{\sigma}_R^z + \cos^2(\alpha/2) \hat{\sigma}_R^- + \sin^2(\alpha/2) \hat{\sigma}_R^+ \quad (22)$$

$$\hat{\sigma}^z = \cos \alpha \hat{\sigma}_R^z - i \sin \alpha \hat{\sigma}_R^+ + i \sin \alpha \hat{\sigma}_R^-. \quad (23)$$

The expressions should be plugged into the Hamiltonian of the Heisenberg chain in a magnetic field. The spin wave approximation then consists in using boson operators related to the local spin operators as follows:  $\hat{\sigma}_R^+ = a$ ,  $\hat{\sigma}_R^- = a^+$  and  $\hat{\sigma}_R^z = 1 - 2a^+a$ . Technically, the effect of the rotation to the local framework is to eliminate linear terms in boson operators. We are thus left with a hamiltonian that is quadratic in terms of Holstein–Primakov bosons. Considering only two consecutive spins with boson operators  $a$  and  $b$ , and after straightforward calculations, we obtain the following spin wave Hamiltonian

$$H^{(sw)} = \frac{J_\perp}{2} (a^+a + b^+b) + \frac{J_\perp}{2} \sin^2 \alpha (a^+b^+ + ab) + \frac{J_\perp}{2} \cos^2 \alpha (ab^+ + a^+b). \quad (24)$$

After Fourier transforming the chain Hamiltonian and performing a Bogoliubov rotation, we deduce the following spin wave spectrum  $\omega_{qz}^2 = A_{qz}^2 - B_{qz}^2$  with

$$A_{qz}^{(\perp)} = J_\perp (1 + \cos^2 \alpha \cos q_z) \quad (25)$$

$$B_{qz}^{(\perp)} = J_\perp \sin^2 \alpha \cos q_z. \quad (26)$$

This expression is defined on the unfolded Brillouin zone  $[-\pi, \pi]$ . However, one should remember that, because of the doubling of the unit cell, the “true” Brillouin zone is  $[-\pi/2, \pi/2]$ . In order to come back from the unfolded Brillouin zone  $[-\pi, \pi]$  to the “true” Brillouin zone  $[-\pi/2, \pi/2]$ , one should consider two spin wave modes for a given wave vector. Notice also that the unfolded dispersion relation is not unique: starting from two distinct spin wave modes in the “true” Brillouin zone, there are two ways to unfold the dispersion relation to the  $[-\pi, \pi]$  interval. The spectrum defined by (25) and (26) corresponds only to one of the unfolding procedures. The other unfolding procedure corresponds to changing  $q_z$  into  $q_z + \pi$  in the unfolded Brillouin zone.

We notice that, in a zero magnetic field, there are two Goldstone modes. As the magnetic field is switched on, one of these Goldstone modes acquires a gap while the other one remains massless (rotations around the magnetic field). The dispersion relation defined by (25) and (26) is thus consistent with the fact that, at the classical level in the presence of a non zero magnetic field the classical ground state is defined up to a rotation around the magnetic field, thus leading a single gapless mode at the spin wave level.

We have rederived the spin wave spectrum defined by (25) and (26) using a method based on the semiclassical equations of motion, which lead exactly to the same result. We do not present here these calculations since they do not lead to new physical insights.

In order to come back to the multilayer problem, we have to take into account the existence of in-plane ferromagnetism, leading to an additional  $A$  term that should be added to (25):

$$A_q^{(\parallel)} = J_{\parallel} (2 - \cos q_x - \cos q_y). \quad (27)$$

Now, if  $h > 2J_{\perp}$ , the spins are aligned with the magnetic field. The dispersion relation is straightforwardly found to be

$$\omega_q = h - J_{\perp} + J_{\perp} \cos q_z + J_{\parallel} (2 - \cos q_x - \cos q_y). \quad (28)$$

This leads to a gap  $\Delta = h - 2J_{\perp}$ .

We have thus obtained an analytic expression for the spin wave spectrum in the absence of dipolar interactions and anisotropy. The evolution of the dispersion relation for  $q_x = q_y = 0$  as a function of  $q_z$  and the magnetic field is plotted on figure 1.

We emphasize that this result does not depend on the direction of the magnetic field: since the Hamiltonian without magnetic field is spin rotational invariant, the spin wave spectrum should be the same whatever the direction of the magnetic field.

### 4.3 Specific heat without dipolar interactions and anisotropy

The specific heat per spin is obtained from the dispersion relation via

$$c_v = \frac{1}{4T^2} \int d\mathbf{q} \frac{\omega_{\mathbf{q}}^2}{\sinh^2(\beta\omega_{\mathbf{q}}/2)}, \quad (29)$$

where  $\beta = 1/T$  is the inverse temperature. We calculated numerically the spin wave specific heat as a function of a magnetic field for a low temperature  $T = 3K$ . The result is plotted on the curve (a) of figure 2. We observe the existence of two regimes: (i)  $h < h_c = 2J_\perp$ : the specific heat is slowly decaying as the magnetic field is increased. We attribute this slow decay to the fact that the system remains gapless in the presence of the magnetic field. If  $h = 0$ , there are two Goldstone modes. One of these Goldstone modes becomes massive as the magnetic increases, leading to a decrease of the low energy density of states and thus a slow decrease in the specific heat. (ii)  $h > h_c$ : the system acquires a gap  $\Delta = h - 2J_\perp$ , leading to a decay to zero of the specific heat as the magnetic field increases, with a cross-over magnetic field  $h^* = 2J_\perp + T$ .

#### 4.4 Spin wave spectrum in the presence of in-plane dipolar interactions

We now assume the existence of in-plane dipolar interactions. This assumption is motivated by the fact that the ferromagnetic layers are separated by paramagnetic layers, and it is thus reasonable to suppose that only spins in the same layer are coupled by dipolar interactions.

The first step is to calculate the zero temperature classical configuration of spins. This can be easily done by minimizing the classical energy with respect to the canting angle and we find

$$\cos \alpha = \frac{h}{2J_\perp + 3\pi J_d} \quad (30)$$

in the regime where the spins are canted. Physically, we expect that, at the classical level, the effect of dipolar interactions is to open the canted angle since dipolar interactions play in favor of attracting the spins in the planes. This is indeed the case, as shown by equation (30). Notice that in the evaluation of the dipolar interaction energy, we have replaced the discrete summation over the lattice by an integral. We will use this approximation throughout this paper to treat the effects of long range in-plane dipolar interactions.

Next, we need to calculate the spin wave spectrum in the presence of dipolar interactions. The calculations are lengthly but straightforward so that we just give here the results. The idea consists in eliminating linear Holstein–Primakov bosons by a rotation to the local framework. Keeping only the quadratic terms in boson operators leads to the following results in the canted phase. The additional contribution to the  $A_q$  term due to dipolar interactions is

$$A_q^{(dip)} = \frac{3\pi J_d}{2} \cos^2 \alpha + \pi J_d \left( I_0(q_\parallel) - 1 \right) + \frac{3\pi J_d}{4} I_0(q_\parallel) \left( 3 \sin^2 \alpha - 2 \right) + \frac{9\pi J_d}{4} \sin^2 \alpha \cos(2\phi_q) I_2(q_\parallel), \quad (31)$$

where  $\phi_q$  is the angle between the vector  $(q_x, q_y)$  and the  $x$  axis, and  $I_n$  is expressed in terms of Bessel functions as

$$I_n(q) = \int_1^{+\infty} \frac{dr}{r^2} J_n(qr). \quad (32)$$

The dipolar contribution to the  $B_q$  terms is

$$B_q^{(dip)} = -\frac{3\pi J_d}{4} \left( \sin^2 \alpha I_0(q_\parallel) - \cos(2\phi_q) I_2(q_\parallel) \left( (1 + \cos^2 \alpha) - 2i \cos \alpha \right) \right). \quad (33)$$

As expected, if  $q_x = q_y = 0$ ,  $|A_0^{(dip)}| = |B_0^{(dip)}|$  since the  $q_x = q_y = 0$  mode in a single ferromagnetic layer with dipolar interactions is gapless. Notice that the contribution (33) is in general a complex number. However, this is not a problem: using a phase transformation on the Holstein–Primakov bosons, we show that the spin wave spectrum is given by  $\omega_q^2 = (A_q^{tot})^2 - |B_q^{tot}|^2$ , where the subscript “tot” refers to the total  $A$  and  $B$  terms (the contributions of ferromagnetic in–plane exchange terms + antiferromagnetic coupling terms + dipolar interaction terms have been added). Specializing the dispersion relation to the  $q_x = q_y = 0$  case, and in the absence of a magnetic field ( $\alpha = \pi/2$ ), we observe the existence of two Goldstone modes in the absence of dipolar interactions but in the presence of dipolar interactions, only one of these modes remains massless whereas the other one acquires a gap. This remaining massless mode corresponds to rotations of the classical spins inside the planes. In the presence of a magnetic field, this massless mode remains since it also corresponds to the rotation of the spins around the magnetic field (perpendicular to the planes).

Notice also that the terms proportional to  $I_2(q_{\parallel})$  in (31) and (33) are expected to lead to a very small (and neglectable) contribution to the specific heat: the main contribution to the specific heat comes from the lowest energy states, namely the states next to  $q_x = q_y = 0$ . Along this line, the terms proportional to  $I_2$  vanish since  $I_2(0) = 0$ . In the rest of the Brillouin zone the contribution of the terms involving  $I_2$  remains very small compared to the in–plane ferromagnetic exchange term, since  $J_{\parallel}$  is two orders of magnitude larger than  $J_d$ . In the present case of a perpendicular magnetic field, the terms proportional to  $I_2$  can be treated exactly since they are the same for all types of layers (invariance under the  $\alpha \rightarrow -\alpha$  transformation). As we shall see below, this is not the case for a magnetic field parallel to the layers. However, we will argue that one can safely neglect these terms since they lead to a neglectable contribution to the specific heat.

The dispersion relation on the line  $q_x = q_y = 0$  as a function of  $q_z$  and the magnetic field is plotted on figure 3.

#### 4.5 Magneto crystalline anisotropy as a pseudo dipolar interaction

We now take into account an anisotropy term (4), under the form of a pseudo dipolar in–plane interaction. We just give the results. One should first calculate the canting angle in the presence of such an interaction. After minimizing the classical energy, we find easily

$$\cos \alpha = \frac{h}{2J_{\perp} + 3\pi J_d/2 - 3K}. \quad (34)$$

This equation is consistent with the fact that the pseudo–dipolar interactions play in favor of aligning the spins perpendicular to the layers, and thus reduce the canting angle. As far as the spin wave spectrum is concerned, the first effect of these pseudo–dipolar interactions is to renormalize  $J_{\parallel}$ :  $J_{\parallel} \rightarrow J_{\parallel} - K$ . Since  $K$  is much smaller than  $J_{\parallel}$ , this effect is very small. The contribution of the

anisotropy to  $A$  is found to be

$$A_q^{(K)} = -3K + \frac{3K}{2} \left( \cos q_x + (\cos^2 \alpha) \cos q_y \right), \quad (35)$$

and the contribution to  $B$  is

$$B_q^{(K)} = \frac{3K}{2} \left( \cos q_x - (\cos^2 \alpha) \cos q_y \right). \quad (36)$$

As in the case of dipolar interactions,  $|A_0^{(K)}| = |B_0^{(K)}|$  if  $q_x = q_y = 0$  since the  $q_x = q_y = 0$  mode is a Goldstone mode of a ferromagnetic layer with pseudo-dipolar interactions. Figure 4 shows the dispersion relation along the line  $q_x = q_y = 0$  as a function of  $q_z$  and the magnetic field. Qualitatively, adding an anisotropy term does not change the main features of the dispersion relation (namely the existence of a single massless Goldstone mode).

#### 4.6 Specific heat in the presence of in-plane dipolar interactions and magneto crystalline anisotropy

We are now in position to calculate the variations of the low temperature specific heat as a function of the intensity of a magnetic field applied perpendicular to the layers, within the spin wave approximation for the Hamiltonian (2)(3)(4). These variations are plotted on the curve (b) of figure 2. We observe two regimes: (i) for  $h < h_c = 2J_\perp + 3\pi J_d - 3K$ , we observe that the specific heat increases as the magnetic field increases. We attribute this behavior to the fact that increasing the magnetic field induces an increase of the low energy density of states. This can be seen as follows. If  $q_x = q_y = 0$ , the dispersion relation around the Goldstone mode  $q_z = \pi - \Delta q_z$  (in the unfolded Brillouin zone) is of the form

$$\omega_{q_x=0, q_y=0, q_z=\pi-\Delta q_z} = \lambda \sin \alpha \Delta q_z. \quad (37)$$

with  $\lambda$  independent on the magnetic field:

$$\lambda^2 = J_\perp \left( J_\perp + \frac{3\pi J_d}{2} - \frac{3K}{2} \right). \quad (38)$$

The density of states in the vicinity of the massless mode is thus an increasing function of the magnetic field, leading to an increase of the specific heat as the magnetic field increases.

(ii)  $h > h_c$ : the gap is  $\Delta = h - h_c$  thus leading to a decrease to zero of the specific heat as the magnetic field increases with a cross-over magnetic field  $h^* = T + h_c = T + 2J_\perp + 3\pi J_d/2 - 3K$ .

Finally, we can compare this result with the specific heat in the absence of dipolar interactions. In a zero magnetic field, we expect the specific heat without dipolar interactions and anisotropy to be larger than the specific heat with dipolar interactions and anisotropy since there is a single massless mode in the former case and two massless modes in the latter. This is indeed the case, as shown on figure 2. Now, consider the aligned state ( $h > h_c$ ). The gap is reduced when dipolar and pseudodipolar interactions are switched on, so that switching on dipolar interactions and anisotropy

should increase the specific heat, which is what is observed on figure 2. The existence of a crossing point between the specific heat curves with and without dipolar interactions and anisotropy on figure 2 is thus consistent with our qualitative analysis.

## 5 Spin wave theory in a longitudinal magnetic field

We now examine the case of a magnetic field applied parallel to the layers. The effect of the orientation of the magnetic field can only be seen when dipolar interactions and anisotropy are taken into account. Namely, in the absence of dipolar interactions and anisotropy, the spin wave spectrum is the one calculated in section 4.2. We are going to calculate the effects of a longitudinal magnetic field. To do so, we use the same technique as in section 4.2: we first express the Hamiltonian in terms of the spin operators quantized along the local magnetization axis, which leads to a quadratic Hamiltonian at the spin wave level, that can be diagonalized via a Fourier transform and a Bogoliubov transformation. First, we treat the problem in the absence of dipolar interactions and anisotropy with the spins in the planes direction. Of course, we recover the results of section 4.2. In a second step, we discuss the effects of in-plane dipolar interactions and anisotropy. In order to avoid confusion with the previous calculations, we call  $\varphi$  the canting angle.

### 5.1 Spin wave spectrum in the absence of dipolar interactions and anisotropy

If  $\mathbf{w}$  denotes the unit vector of coordinates  $\mathbf{w}(\sin \varphi, \cos \varphi, 0)$ , with  $\varphi$  the canting angle, then, the local spin states in a given layer are

$$|+\rangle_R = \frac{1}{\sqrt{2}} (|+\rangle + e^{-i\varphi} |-\rangle) \quad (39)$$

$$|-\rangle_R = \frac{1}{\sqrt{2}} (-e^{i\varphi} |+\rangle + |-\rangle), \quad (40)$$

where we have performed a rotation of  $\pi/2$  around the  $\mathbf{w}$  axis. The case of the other type of layer is obtained by replacing  $\varphi$  by  $-\varphi$  in these equations. The expression of the spin operators  $\hat{\sigma}^{\pm,z}$  in terms of the local spin operators  $\hat{\sigma}_R^{\pm,z}$  is

$$\hat{\sigma}^+ = \frac{1}{2} (e^{-i\varphi} \hat{\sigma}_R^z + \hat{\sigma}_R^+ - e^{-2i\varphi} \hat{\sigma}_R^-) \quad (41)$$

$$\hat{\sigma}^- = \frac{1}{2} (e^{i\varphi} \hat{\sigma}_R^z + \hat{\sigma}_R^- - e^{2i\varphi} \hat{\sigma}_R^+) \quad (42)$$

$$\hat{\sigma}^z = -e^{i\varphi} \hat{\sigma}_R^+ - e^{-i\varphi} \hat{\sigma}_R^-. \quad (43)$$

Using the same technique as in section 4.2, we express the Hamiltonian of a single a-b link in terms of the  $a$  and  $b$  bosons (one type of boson for each direction of the classical ground state). In order to get rid of phase factors, one has to define new boson operators  $\tilde{a} = a \exp(i\varphi)$  and  $\tilde{b} = b \exp(-i\varphi)$ . We then recover the spin wave Hamiltonian (24) in terms of the  $\tilde{a}$  and  $\tilde{b}$  bosons.

## 5.2 Spin wave contribution of in-plane dipolar interactions

The first step is to determine the classical spin configurations. In the presence of dipolar interactions, the classical spins are aligned in the planes, with a canting angle

$$\cos \varphi = \frac{h}{2J_{\perp}}. \quad (44)$$

Notice that the dipolar interaction coupling  $J_d$  does not come into account in the expression of the canting angle. This is due to the fact that the spins are in the planes, and therefore the classical energy of dipolar interactions is a constant, independent on the canting angle  $\varphi$ . This is already a first difference between the cases of a perpendicular and longitudinal magnetic fields.

The second step is to include in-plane dipolar interactions at the spin wave level. We do not give the details of the calculations. The contribution of dipolar interactions to  $A$  for a given layer is

$$A_q^{(dip)} = \pi J_d \left( I_0(q_{\parallel}) - 1 \right) + \frac{3\pi J_d}{4} I_0(q_{\parallel}) - \frac{9\pi J_d}{4} \cos(2(\phi_q - \varphi)) I_2(q_{\parallel}), \quad (45)$$

and the contribution to  $B$  is

$$B_q^{(dip)} = \frac{3\pi J_d}{4} \left( I_0(q_{\parallel}) + \cos(2(\phi_q + \varphi)) I_2(q_{\parallel}) \right). \quad (46)$$

These calculations have been carried out in a given layer. The main problem regarding these expressions is that they are not invariant under the  $\varphi \rightarrow -\varphi$  transformation. In other words, the dipolar terms induce a hybridization between the two Goldstone modes in the  $[-\pi/2, \pi/2]$  Brillouin zone. However the strength of the hybridization is proportional to  $I_2(q_{\parallel})$ . As mentioned earlier, we expect the terms proportional to  $I_2$  to lead to a really small contribution to the specific heat since i)  $I_2$  vanishes along the line  $q_x = q_y = 0$ , where the lowest energy modes are located ii) outside the  $q_x = q_y = 0$  line, these terms are dominated by the ferromagnetic exchange interaction which is two orders of magnitude larger than the dipolar coupling. We can thus safely neglect the terms proportional to  $I_2$  in our specific heat calculation.

Finally, in the presence of dipolar interactions, the results in a perpendicular and longitudinal magnetic field should be the same in the limit of vanishing fields. This is indeed the case. In order to get the same result for  $\alpha = \varphi = \pi/2$ , one should make a  $\pi$  shift on the  $z$  component of the wave vector. This  $\pi$  shift is allowed since, as mentioned earlier, there are two possibilities of unfolding the “true” Brillouin zone  $[-\pi/2, \pi/2]$  to the extended Brillouin zone  $[-\pi, \pi]$ . These two possibilities are precisely related to each other by a  $\pi$  shift on the  $z$  component of the wave vector.

Before discussing the results (45) and (46), we would like to include the effects of an anisotropy.

## 5.3 Spin wave contribution of the magneto crystalline anisotropy as a pseudo-dipolar interaction

The magnitude of the anisotropy is chosen to be small enough so that the classical configuration of spins is aligned in the plane, whatever the value of the longitudinal magnetic field. Under this

assumption, the canting angle is given by (44) and is independent on the strength  $K$  of the anisotropy. The anisotropy term can straightforwardly be incorporated in the spin wave approach. The results are as follows. The first effect of the anisotropy is a renormalization of  $J_{\parallel}$ :  $J_{\parallel} \rightarrow J_{\parallel} - K$ . This effect is very small since  $J_{\parallel}$  is two orders of magnitude larger than  $K$ . The contribution of the anisotropy to the  $A$  term is

$$A^{(K)} = -3K + \frac{3K}{2} (\sin^2 \varphi \cos q_x + \cos^2 \varphi \cos q_z). \quad (47)$$

The contribution of the anisotropy to the  $B$  term is

$$B^{(K)} = -\frac{3K}{2} (\sin^2 \varphi \cos q_x + \cos^2 \varphi \cos q_z). \quad (48)$$

The dispersion relation in the presence of an anisotropy and dipolar interactions is plotted on figure 5 in the extended Brillouin zone for  $q_x = q_y = 0$ . In a zero magnetic field, we observe the presence of a massless mode associated to the rotation of the spins inside the planes. As soon as a magnetic field is switched on, this mode acquires a gap, due to the fact that the magnetic field breaks the rotational invariance of the ground state with respect to in-plane rotations. Another effect is that if  $h = 2J_{\perp}$ , we observe the existence of a massless mode. The existence of this gapless mode can be understood at the classical level as follows: consider a magnetic field strictly equal to  $2J_{\perp}$ . It is then possible to calculate the energy of a classical spin wave of amplitude  $\theta$  around the aligned state, and expand the energy in powers of the amplitude  $\theta$  of the classical spin wave. One then get the result that the leading term in this expansion is of order  $\theta^4$ . More precisely, the energy per spin of an antiferromagnetic classical spin wave of amplitude  $\theta$  around the aligned state ( $h \geq 2J_{\perp}$ ) is

$$E(\theta) = -\frac{h}{2} \cos \theta + \frac{J_{\perp}}{4} \cos(2\theta) = -\frac{1}{4}(h - 2J_{\perp})(1 - \theta^2) - \frac{1}{48}(h - 8J_{\perp})\theta^4 + \dots \quad (49)$$

If  $h = 2J_{\perp}$  the leading term of this expansion is of order  $\theta^4$ , thus leading to a flat mode at the harmonic order. It is thus not surprising that at the quantum spin wave level one finds a gapless mode right at the canting transition.

#### 5.4 Specific heat in a longitudinal magnetic field

The specific heat in a longitudinal magnetic field is plotted on the curve (c) of figure 2. We observe the same type of variations as in the perpendicular magnetic field case, except that the specific heat with an in-plane magnetic field is smaller than the specific heat without dipolar interactions and anisotropy. This can be explained qualitatively as follows. In the aligned state ( $h > 2J_{\perp}$ ), the gap is given by

$$\Delta^2 = (h - 2J_{\perp})^2 + (h - 2J_{\perp}) \left( \frac{3\pi J_d}{2} - 3K \right), \quad (50)$$

where the dispersion relation has been specialized to the  $q_x = q_y = 0, q_z = \pi$  case. As a consequence, the gap with an in-plane magnetic field and dipolar interactions and anisotropy is larger than in the absence of dipolar interactions and anisotropy. We thus expect from this argument a lower specific heat, which is indeed the case as observed on figure 2.

## 6 Conclusion and discussion

Let us now summarize our results. We have calculated the spin wave contribution to the specific heat in three different cases: (a) without dipolar interactions and anisotropy. At this level of approximation, the specific heat does not depend on the direction of the magnetic field since the Hamiltonian without a magnetic field is spin rotational invariant. (b) with dipolar interactions and anisotropy for a perpendicular applied magnetic field. (c) with dipolar interactions and anisotropy for a longitudinal applied magnetic field. In case (b), the location of the canting transition depends explicitly on the strength of dipolar interactions and anisotropy. In case (c), the location of the canting transition is independent on the strength of dipolar interactions and anisotropy. We observe a maximum of the specific heat at the canting transition in cases (b) and (c). Another conclusion is that, due to the anisotropy of the system, we predict an anisotropy in the specific heat. Namely, the specific heat in a perpendicular magnetic field is larger than the specific heat in an in-plane magnetic field.

However, there is also a contribution to the specific heat due to non magnetic interlayers. As only a few percentage of their conduction electrons is polarized by the exchange coupling [16] the interlayers should behave nearly as a bulk paramagnet. This paramagnetic contribution per spin has then the form

$$c_v^{(para)} = \frac{(\beta h)^2}{\cosh^2(\beta h)}, \quad (51)$$

where  $\beta$  is the inverse temperature. This paramagnetic contribution is much larger than the spin wave contribution which is a source of experimental difficulty. Clearly, the sample should be processed in such a way as to minimize the number of paramagnetic atoms.

### Acknowledgements

We would like to thank Monique Giroud for useful discussions. R.M. acknowledges discussions with M. Fabrizio. R.M. also acknowledges the hospitality of NEC Research Institute at Princeton and CRTBT at Grenoble where part of this job was done.

## References

- [1] M.N. Baibich, J.M. Broto, A. Fert, Van Dau F. Nguyen, F. Petroff, P. Etienne, P. Creuzet, A Friederich and J. Chazelas, Phys. Rev. Lett. 61 (1988) 2472
- [2] S.S.P. Parkin, Phys. Rev. Lett. 67 (1991) 3598; S.S.P. Parkin, Z.G. Li and D.J. Smith, Appl. Phys. Lett. 54 (1991) 2170; S.S.P. Parkin, N. More and K.P. Roche, Phys. Rev. Lett. 64, 2304 (1990); B. Rodmacq, B. George, M. Vazzadeh and P. Mangin Phys. Rev. B 46 (1992) 1206; E. Vélu, C. Dupas, D. Renard, J.P. Renard and J. Seiden, Phys. Rev. B 46 (1992) 1206.
- [3] *Magnetism and Structure in Systems of Reduced Dimension* Edited by R.F.C. Farrow et al., Nato ASI Series B: Physics Vol. 309.
- [4] B. Heinrich and J.F. Cochran, Advances in Physics, 1993, 42, nr. 5, 523-639.
- [5] D.W. Denlinger, E.N. Abarra, K. Allen, P.W. Rooney, M.T. Messer, S.K. Watson and F. Hellerman, Rev. Sci. Instrum. 65 (4) 946 (1994) .
- [6] F.Fominaya et al., to be published. The calorimeter has a resolution of pJ/K at 2K in heat capacity measurements in dependence of an external magnetic field.
- [7] J. Kwo, M. Hong, F.J. Di Salvo, J.V. Waszczak and C.F. Majkrzak, Phys. Rev. B 35 (1987) 7925; C.F. Majkrzak, J.W. Cable, J. Kwo, M. Hong, D.B. McWhan, Y. Yafet, J.V. Waszczak and C. Vettier, Phys. Rev. Lett. 56 (1986) 2700.
- [8] R.E. Camley and R.L. Stamps, J. Phys.: Condens. Matter 5 (1993) 3727.
- [9] P. Bruno, Phys. Rev. B 43, 6015 (1991).
- [10] As the thickness of the ferromagnetic layers is increased, the strength of dipolar interactions  $J_d$  increases whereas the anisotropy  $K$  remains the same.
- [11] T. Holstein and H. Primakov, Phys. Rev. Lett. 58, 1098 (1940).
- [12] I. Affleck, J. Phys. 1, 3047 (1989).
- [13] *Introduction to Solid State Physics*, C. Kittel, sixth edition (1986), J. Wiley and Sons.
- [14] W. Folkers, J.M.M.M. 94 (1991) 302.
- [15] W. Folkers and S.T. Purcell, J.M.M.M. 111 (1992) 306.
- [16] S. Staehler, G. Schütz, P. Fisher, M. Knüller, S. Rüegg, S. Parkin, H. Ebert and W.B. Zeper, J.M.M.M. 121 (1993) 234.

## Figure captions

Figure 1:

Dispersion relation as a function of the magnetic field. The dispersion relation is plotted along the line  $q_x = q_y = 0$  as a function of the strength of the magnetic field in the extended Brillouin zone  $[-\pi, \pi]$ . There is no dipolar interaction nor exchange interaction. We took  $J_{\perp} = 1$ .

Figure 2:

Specific heat per spin in the different cases considered in this article, with  $J_{\perp} = 1K$ ,  $J_{\parallel} = 100K$ , and as a function of the external magnetic field. The curve (a) corresponds to the specific heat in the absence of dipolar interactions and anisotropy. (b) corresponds to a perpendicular applied magnetic field, with  $J_d = 1K$  and  $K = 0.5K$ . (c) corresponds to a longitudinal magnetic field with  $J_d = 1K$  and  $J_{\perp} = 0.5K$ .

Figure 3:

Dispersion relation as a function of the intensity of a perpendicular magnetic field. The dispersion relation is plotted along the line  $q_x = q_y = 0$  as a function of the strength of the magnetic field in the extended Brillouin zone  $[-\pi, \pi]$ . We took  $J_{\perp} = 1$ ,  $J_d = 1$  and  $K = 0$ . Notice the differences with figure 1.

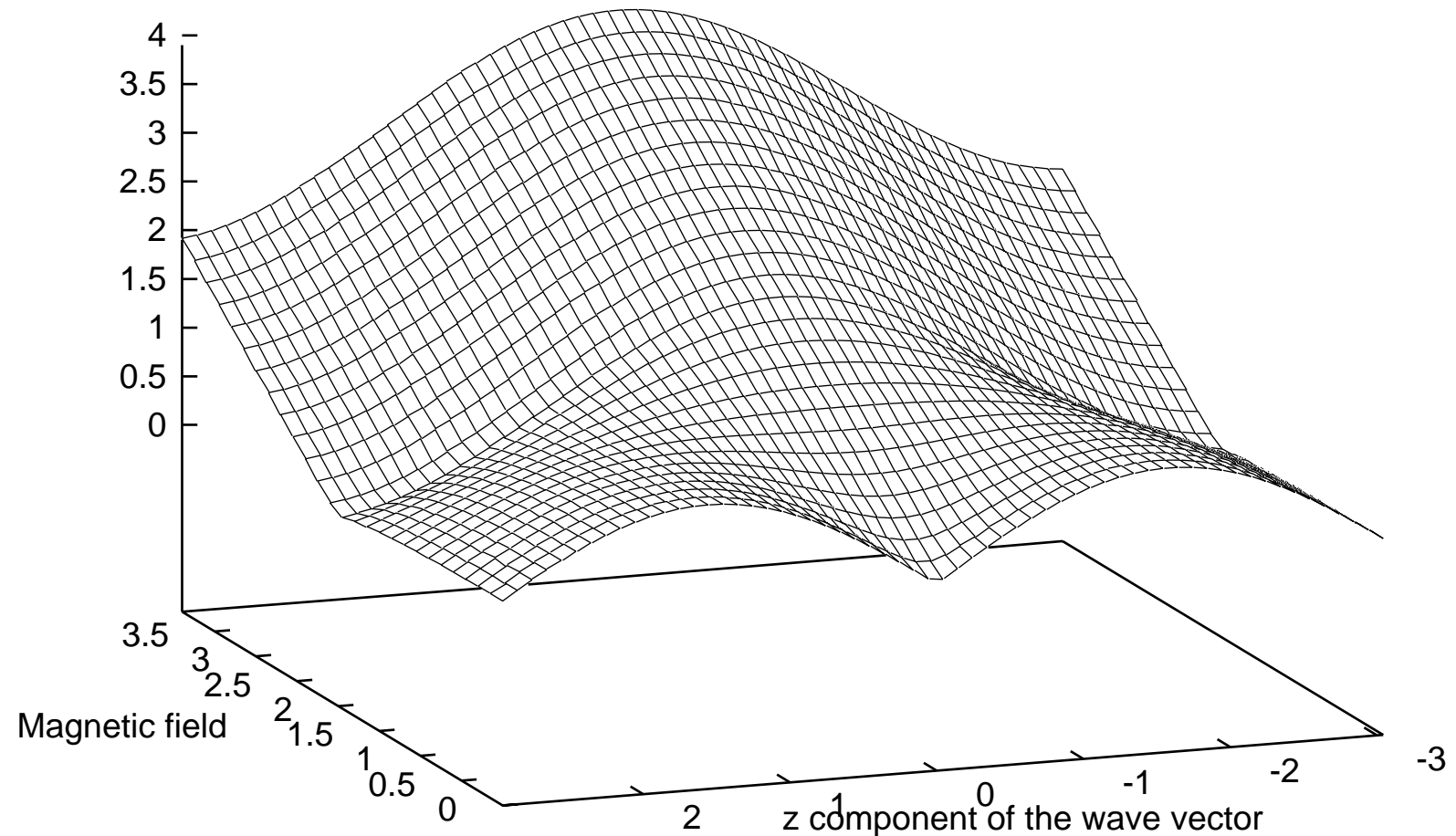
Figure 4:

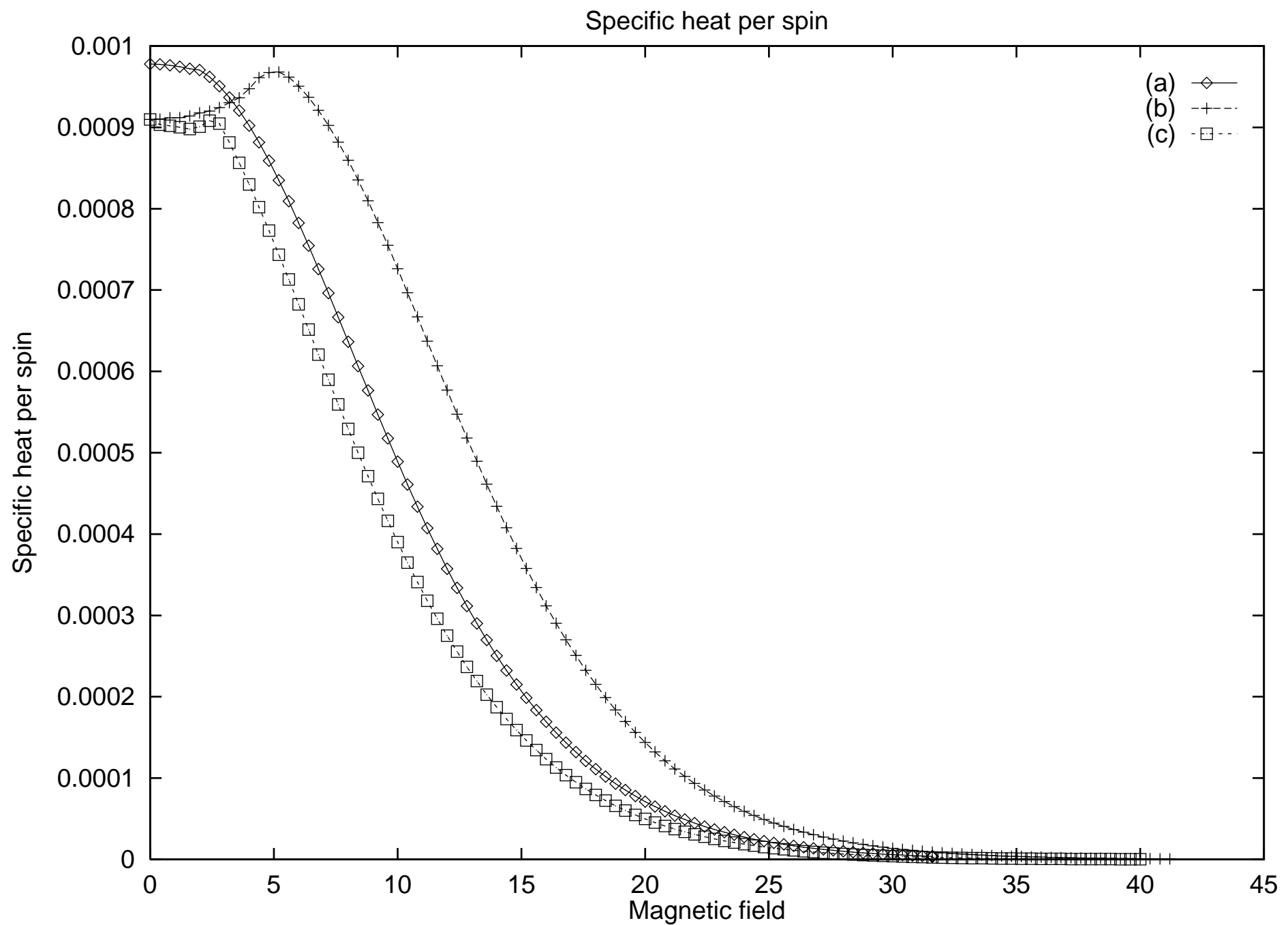
Dispersion relation as a function of the intensity of a perpendicular magnetic field. The dispersion relation is plotted along the line  $q_x = q_y = 0$  as a function of the strength of the magnetic field in the extended Brillouin zone  $[-\pi, \pi]$ . We took  $J_{\perp} = 1$ ,  $J_d = 1$  and  $K = 0.5$ . The variations of the dispersion relation are very similar to the ones of figure 3 where  $K$  was set to zero.

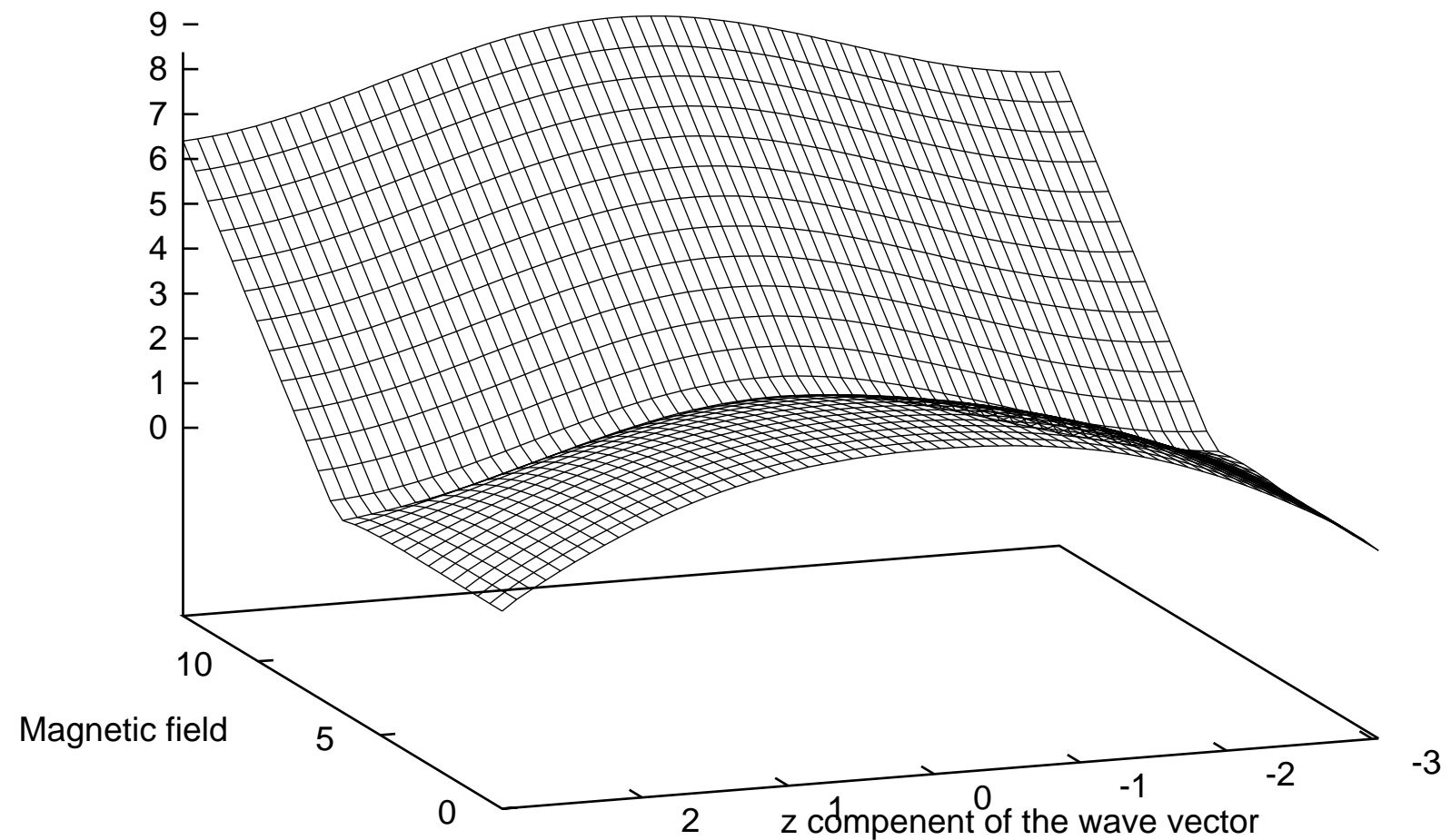
Figure 5:

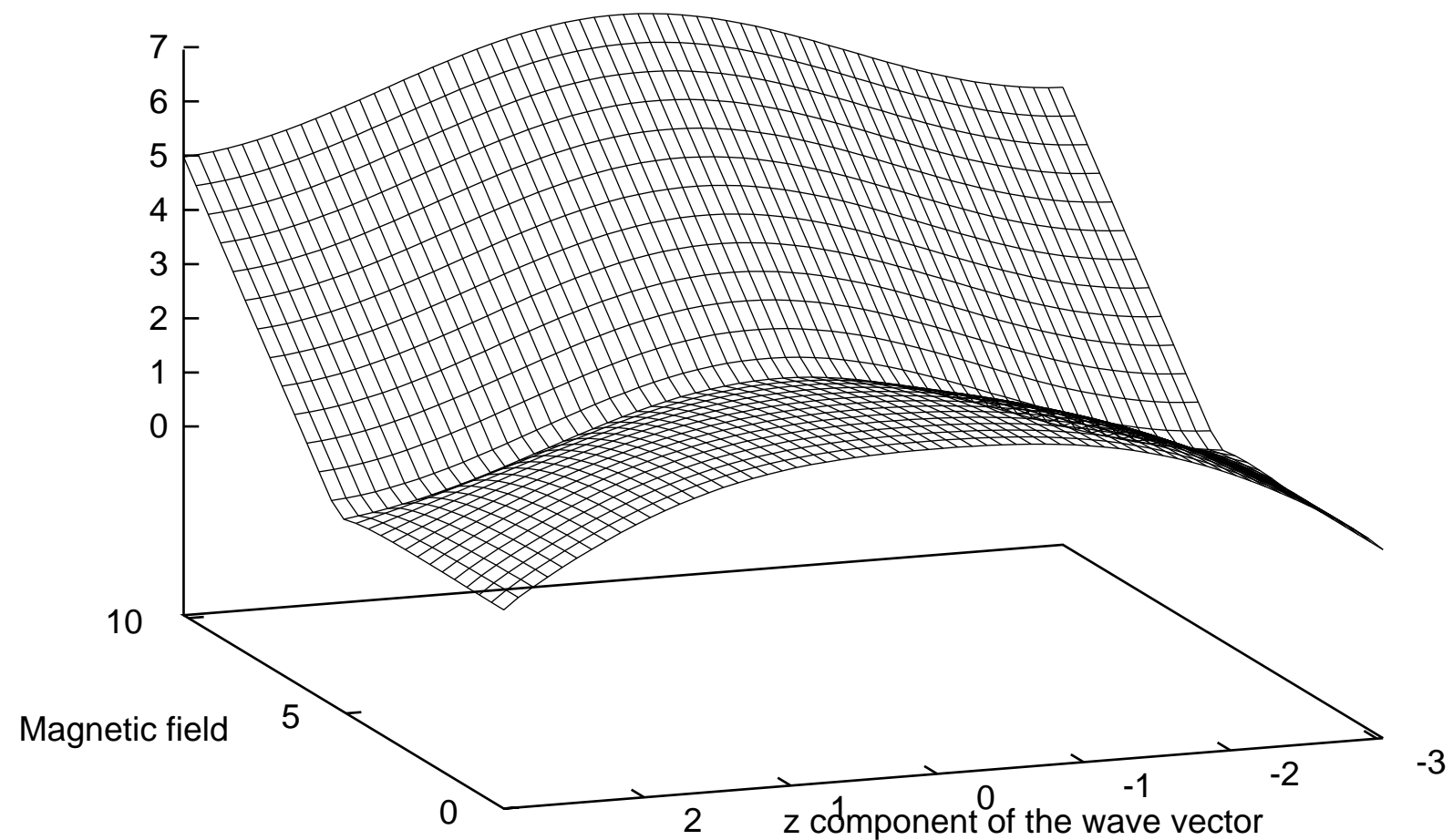
Dispersion relation as a function of the intensity of a longitudinal magnetic field. The dispersion relation is plotted along the line  $q_x = q_y = 0$  as a function of the strength of the magnetic field in the extended Brillouin zone  $[-\pi, \pi]$ . We took  $J_{\perp} = 1$ ,  $J_d = 1$  and  $K = 0.5$ . Notice the differences with figure 1.

## Dispersion relation









Dispersion relation

